Protein Science (1995), *4*:2478–2486. Cambridge University Press. Printed in the USA.

Phosphorylation of serine-46 in HPr, a key regulatory protein in bacteria, results in stabilization of its solution structure

KATHERINE PULLEN,[1] PONNI RAJAGOPAL,[1] BRUCE R. BRANCHINI,[2] MARY ELIZABETH HUFFINE,[4] JONATHAN REIZER,[3] MILTON H. SAIER, JR.,[3] J. MARTIN SCHOLTZ,[4] AND RACHEL E. KLEVIT[1]

[1] Department of Biochemistry and Biomolecular Structure Center, University of Washington, Seattle, Washington 98195-7742
[2] Department of Chemistry, Connecticut College, New London, Connecticut 06320
[3] Department of Biology, University of California at San Diego, La Jolla, California 92093-0116
[4] Departments of Medical Biochemistry and Genetics, and Biochemistry and Biophysics, Texas A&M University, College Station, Texas 77843

(RECEIVED September 20, 1995; ACCEPTED October 5, 1995)

Abstract

The serine-phosphorylated form of histidine-containing protein (HPr), a component of the phosphoenolpyruvate:sugar phosphotransferase system from *Bacillus subtilis*, has been characterized by NMR spectroscopy and solvent denaturation studies. The results indicate that phosphorylation of Ser 46, the N-cap of α-helix-B, does not cause a conformational change but rather stabilizes the helix. Amide proton exchange rates in helix-B are decreased and phosphorylation stabilizes the protein to solvent and thermal denaturation, with a $\Delta\Delta G$ of 0.7–0.8 kcal mol^{-1}. A mutant in which Ser 46 is replaced by aspartic acid shows a similar stabilization, indicating that an electrostatic interaction between the negatively charged groups and the helix macrodipole contributes significantly to the stabilization.

Keywords: NMR; protein dynamics; protein phosphorylation; protein stability; protein structure; PTS; solvent denaturation

Control of cellular processes via reversible protein phosphorylation is ubiquitous in biology. First observed in glycogen phosphorylase (Krebs & Fischer, 1956), hundreds of other examples have since been described in both eukaryotes and prokaryotes. Structural information on how the addition of a phosphate group can dramatically affect protein function is still surprisingly limited—crystal structures have been reported for three proteins that are phosphorylated at a regulatory site: glycogen phosphorylase (Barford & Johnson, 1989), isocitrate dehydrogenase (Hurley et al., 1990), and cAMP-dependent protein kinase (Zheng et al., 1993). In the two cases where crystal structures are also available for unphosphorylated forms of the protein, the effect of phosphorylation is quite different. The polypeptide chain near Ser 14 in native GP is disordered in the crystal, and phosphorylation promotes the formation of ordered structure near the serine as well as long-range tertiary and quaternary conformational changes that affect the function of the enzyme. Ser 113 in IDH is in the N-cap position of an α-helix and phosphorylation yields only small local changes in structure. Thus, the two available examples illustrate two different mechanisms by which phosphorylation modulates function. Although the structure of unphosphorylated cAPK has not been solved, structures of related protein kinases in their unphosphorylated forms suggest that phosphorylation of Ser 338 will result in a large movement of a flexible loop near the active site (Cox et al., 1994).

The bacterial phosphoenolpyruvate:sugar phosphotransferase system mediates concomitant transport and phosphorylation of exogenous sugars. The PTS also controls the phenomena of inducer exclusion, inducer expulsion, and catabolite repression in bacteria (Postma et al., 1993; Deutscher et al., 1994; Ye et al., 1994). In Gram-positive bacteria, the central regulatory protein

Reprint requests to: Rachel E. Klevit, Department of Biochemistry and Biomolecular Structure Center, Box 357742, University of Washington, Seattle, Washington 98195-7742; e-mail: klevit@u.washington.edu.

Abbreviations: HPr, histidine-containing protein; HPr(Ser-P), HPr phosphorylated on Ser 46; HPr(His-P), HPr phosphorylated on His 15; EI, enzyme I; EIIA, enzyme IIA; PTS, phosphoenolpyruvate:sugar phosphotransferase system; 2D and 3D, two- and three-dimensional; NOESY, nuclear Overhauser enhancement spectroscopy; HMQC, heteronuclear multiple quantum correlation; TOCSY, total correlation spectroscopy; PEP, phosphoenolpyruvate; P.E. COSY, primitive-exclusive coherence spectroscopy; GP, glycogen phosphorylase; IDH, isocitrate dehydrogenase; cAPK, cyclic-AMP-dependent protein kinase.

is histidine-containing protein, a small phosphoryl transfer protein that can be phosphorylated either on a catalytic histidine (His 15) by a PEP-dependent protein kinase, or on a regulatory serine (Ser 46) by an ATP-dependent protein kinase (Reizer et al., 1984, 1992).

HPr(Ser-P) interacts with a remarkably wide variety of proteins to control their activities, whereas neither the unphosphorylated form of HPr nor HPr(His-P) bind to these target proteins (Deutscher et al., 1995; Ye & Saier, 1995). The precise molecular basis for this selective binding is unknown, but it undoubtedly reflects electrostatic and/or conformational changes that accompany phosphorylation of HPr at Ser 46. Thus, definition of the structural features that accompany HPr(Ser) phosphorylation represents a key step toward understanding the regulatory mechanisms involving this pivotal protein.

Here we report a detailed characterization of the effects of serine phosphorylation on the structure and stability of HPr by NMR and solvent denaturation studies. Structural information is available both from crystallographic (Herzberg et al., 1992) and NMR studies (Wittekind et al., 1992) of the native protein, making HPr an excellent system in which to study the effects of serine phosphorylation on the solution structure and properties of a protein regulated by this type of modification. The solution and crystal structures of HPr both clearly define an antiparallel four-stranded β-sheet flanked on one side by two long α-helices (helices A and C, Fig. 1). Similar to the phosphorylatable serine in IDH, Ser 46 is the N-cap for a third short helix comprising residues 47–53 (helix B, Fig. 1). This helix was ill-defined in the original solution structure; however, recent solution structure calculations based on a significantly larger number of constraints obtained from 3D NOESY spectra confirm the presence of helix-B in solution, although very rapid exchange rates for helix-B amide protons indicate that the short helix is dynamic (B.E. Jones, P. Rajagopal, & R.E. Klevit, unpubl. results).

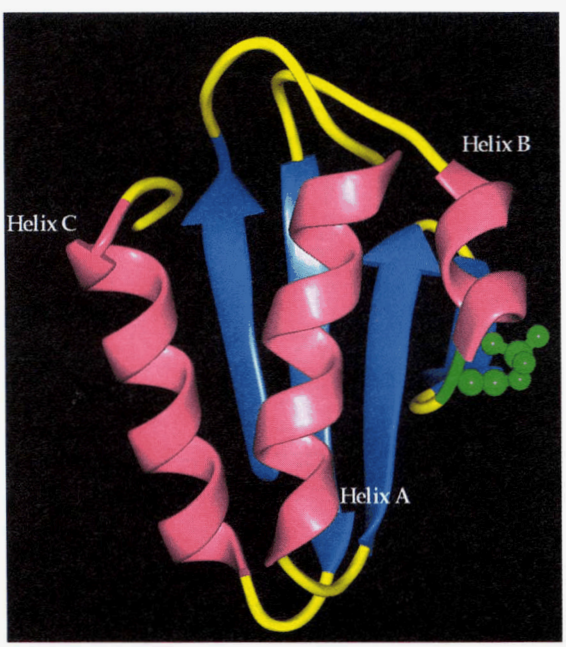

Fig. 1. Ribbon representation of the structure of HPr(Ser-P), highlighting the elements of regular secondary structure (β-strands are blue and α-helices are pink). The phosphoserine residue at position 46 is shown in green ball-and-stick representation.

Results

NMR studies

Table 1 presents a summary of the NMR measurements collected on samples of *Bacillus subtilis* HPr and HPr(Ser-P) under identical conditions. For the majority of resonances, the measured values of chemical shifts, J-coupling constants, NOEs, and amide exchange rates are indistinguishable within experimental uncertainties for the two forms of the protein. Thus, the first major conclusion that can be drawn from the NMR measurements is that, unlike GP but similar to IDH, phosphorylation of Ser 46 does not result in a global conformational change. Changes in backbone conformation would be detected as changes in the $^3J_{NH\alpha}$ coupling constant, which is correlated to the dihedral angle, ϕ (Wüthrich, 1986). No difference in coupling constants greater than two standard deviations from the average difference was detected, even at the site of phosphorylation. Changes in side-chain conformation would be reflected in the coupling patterns of $^3J_{\alpha\beta}$ and $^3J_{N\beta}$, which are sensitive to rotations about the C_α-C_β bond (i.e., χ_1). Ser 46 is the only residue with a difference greater than two standard deviations from the average difference of 0.7 Hz (SD 0.5 Hz): $^3J_{\alpha\beta}$ for (HB2, HB3) are (4.0, 9.3 Hz) and (5.9, 9.9 Hz) in HPr and HPr(Ser-P), respectively. However, both sets of coupling constants are consistent with a χ_1 near the *trans* conformation, and the observed difference in scalar coupling may be due to the covalent modification of the side chain itself. Finally, an exhaustive peak-by-peak comparison of 2D NOESY spectra did not reveal any new or missing cross peaks in the two forms of HPr. A more limited quantitative comparison of 2D NOESY intensities identified only two NOE cross peaks (see below) with significantly different intensities in the two forms of the protein. Thus, NMR parameters that are sensitive to secondary and tertiary structure indicate that HPr does not undergo a conformational change upon its regulatory phosphorylation.

In contrast to the above parameters that report on the disposition of nuclei relative to each other, chemical shifts are sensitive to changes in the chemical and/or electronic environment of a nucleus. As a nucleus becomes more deshielded from the external magnetic field, its resonance will shift downfield. Preliminary ^1H NMR measurements on HPr(Ser-P) revealed that chemical shift perturbations were restricted to a region near Ser 46 in the three-dimensional structure (Wittekind et al., 1989). (^1H, ^{15}N)-HMQC spectra of HPr and HPr(Ser-P) confirm and extend these observations (Fig. 2). Consistent with the absence of conformational change, most of the resonances in the two spectra superimpose. In contrast, resonances in helix-B from residue 47 to 52 experience large ^1H and ^{15}N chemical shift perturbations: 0.20–0.44 ppm in ^1H shifts and 0.5–2.2 ppm in ^{15}N shifts (no other backbone amide resonances change by more than 0.12 ppm for ^1H or 0.5 ppm for ^{15}N). Of these, the resonances of 48, 49, 51, and 52 shift downfield. Five $C^\alpha H$ resonances also shift, four of which are in helix-B, with the largest shift being that of Gly 49 (0.15 ppm downfield). These observations indicate that, although there is no conformational change, the presence of the negatively charged phosphate group

Table 1. *Summary of NMR measurements on HPr and HPr(Ser-P)*[a]

	Chemical shift (ppm)			Coupling constants			Log (protection factor)		
Residue	^{15}N	NH	CαH	$^{3}J_{NH\alpha}$	$^{3}J_{\alpha\beta}$	$^{3}J_{N\beta}$	HPr	HPr (Ser-P)	Sec. Str.[b]
Ala 2			*						
Gln 3	*	*	*		*	*	1.6	1.5	β-A
Lys 4	*	*	*	*	*	*	3.7	3.8	β-A
Thr 5	*	*	*	*			≤2.9	≤2.9	β-A
Phe 6	*	*	*	*	*	*			β-A
Lys 7	*	*	*	*					β-A
Val 8	*	*	*				>3.6	>3.6	β-A
Thr 9	*	*	*	*					
Ala 10	*	*	*	*			≤3.1	≤3.1	
Asp 11	*	*	*	*					
Ser 12		*	*		*				
Gly 13	*	*	*				≤3.5	≤3.5	
Ile 14	*	*	*	*			≤2.3	≤2.3	
His 15	*	*	*	*	*	*			
Ala 16	*	*	*	*					α-A
Arg 17	0.2	*	*						α-A
Pro 18			*		*				α-A
Ala 19	−0.2	*	*				3.0	3.1	α-A
Thr 20	*	*	*	*			3.9	4.0	α-A
Val 21	*	*	*	*			2.4	2.9	α-A
Leu 22	*	*	*	*	*	*	>3.5	>3.5	α-A
Val 23	*	*	−0.06				>3.3	>3.3	α-A
Gln 24	0.3	*	*	*	*	*	>4.1	>4.1	α-A
Thr 25	*	*	*	*			4.0	4.0	α-A
Ala 26	*	*	*	*			>4.4	>4.4	α-A
Ser 27	*	*	*	*					
Lys 28	*	*	*	*	*	*	3.1	3.1	
Tyr 29	*	*	*	*	*	*	>4.0	>4.0	
Asp 30	*	*	*	*					
Ala 31	*	−0.06	*	*					
Asp 32	*	*	*	*	*	*			β-B
Val 33	0.4	−0.08	*						β-B
Asn 34	*	*	*	*	*	*	>4.5	>4.5	β-B
Leu 35	*	*	*	*	*				β-B
Glu 36	*	*	*	*	*	*	>3.5	>3.5	β-B
Tyr 37	*	*	*	*	*	*	>3.8	>3.8	β-B
Asn 38	*	*	*	*	*				
Gly 39	*	*	*						
Lys 40	−0.2	*	*	*					β-C
Thr 41		*	*				≤2.9	≤2.9	β-C
Val 42	*	*	*	*			>3.7	>3.7	β-C
Asn 43	0.2	−0.06	*	*					β-C
Leu 44	−0.3	*	*	*		*	3.7	>3.9	
Lys 45	0.2	0.12	*				≤2.6	3.3	
Ser 46	−0.3	*	−0.12	*	X	*			
Ile 47	1.1	0.20	*	*			1.6	2.0–3.0	α-B
Met 48	−1.2	−0.44	−0.08	*					α-B
Gly 49	−2.2	−0.32	0.04–0.15				1.6	3.3–4.3	α-B
Val 50	0.7	0.24	*	*			≤2.4	3.4	α-B
Val 51	−0.8	−0.06	0.05				≤2.0	2.7	α-B
Ser 52	*	−0.27	*	*	*				α-B
Leu 53	*	*	*	*		*	≤2.6	3.4	α-B
Gly 54	*	*	*				≤2.9	≤2.9	
Ile 55	*	*	*	*			≤2.3	≤2.3	
Ala 56	*	*	*	*			2.9	3.2	
Lys 57		*	*						
Gly 58	*	*	*				≤3.3	≤3.3	
Ala 59	*	*	*	*			>4.4	>4.4	
Glu 60	*	*	*				2.8	2.8	β-D

(*continued*)

Table 1. *Continued*

Residue	Chemical shift (ppm)			Coupling constants			Log (protection factor)		
	^{15}N	NH	CαH	$^{3}J_{NH\alpha}$	$^{3}J_{\alpha\beta}$	$^{3}J_{N\beta}$	HPr	HPr (Ser-P)	Sec. Str.[b]
Ile 61	*	*	*	*			>3.3	>3.3	β-D
Thr 62	*	*	*	*			>3.9	>3.9	β-D
Ile 63	*	*	*	*			>3.7	>3.7	β-D
Ser 64	*	*	*	*	*	*	>3.7	>3.7	β-D
Ala 65	*	*	*	*			>4.5	>4.5	β-D
Ser 66	*	*	*	*	*	*	4.4	4.3	β-D
Gly 67	*	*	*						
Glu 68	*	*	*						
Asp 69	*	*	*	*	*	*	≤2.4	≤2.4	
Glu 70	*	*	*	*			≤2.2	≤2.2	α-C
Asn 71		*	*						α-C
Asp 72	*	*	*	*	*	*	≤2.9	≤2.9	α-C
Ala 73	*	*	*	*			>4.0	>4.0	α-C
Leu 74	*	*	*	*		*	>3.6	>3.6	α-C
Asn 75	*	*	*				>4.5	>4.5	α-C
Ala 76	*	*	*	*					α-C
Leu 77	*	*	*	*			>3.6	>3.6	α-C
Glu 78	*	*	*	*	*		>3.5	>3.5	α-C
Glu 79	*	*	*	*					α-C
Thr 80		*	*				>4.0	>4.0	α-C
Met 81	*	*	*				>4.4	>4.4	α-C
Lys 82	*	*	*	*			>4.3	>4.3	α-C
Ser 83	*	*	*	*	*		≤3.4	≤3.4	α-C
Glu 84	*	*	*			*	2.8	2.8	α-C
Gly 85	*	*	*				≤3.0	≤3.0	
Leu 86	*	*	*	*			3.5	3.5	
Gly 87	*	*	*				≤2.9	≤2.9	
Glu 88	*	*	*		*		3.5	3.3	

[a] Chemical shift and coupling constant measurements. All chemical shifts and coupling constants were measured at 30 °C and at either pH 6.5 or 6.9. Chemical shift differences are calculated as (δ(wt) − δ(HPr(Ser-P)). Therefore, negative values signify a downfield shift upon phosphorylation; *, no significant difference between HPr and HPr(Ser-P); X, significant difference; no entry indicates that a measurement could not be made for one or both forms of the protein. Significance criteria: (1) chemical shifts, difference is greater than the average line width (20 Hz for ^{1}H; 5 Hz for ^{15}N); (2) coupling constants, difference is greater than two standard deviations from the average residue-by-residue difference ($J_{NH\alpha}$ < 5 Hz in both molecules was classified as similar (*); (3) $J_{N\beta}$, different pattern of relative intensities of the two NH to $C^{\beta}H$ cross peaks in HNHB spectra. Due to possible effects of solvent saturation, residues for which no HNHB cross peak was observed are only included if they have a slow amide exchange rate ($t_{1/2}$ > 100 min). Protection factors at 15 °C, pH 6.5, were calculated as described by Bai et al. (1993). The factor for residue 47 in HPr(Ser-P) was calculated using the intrinsic rate for aspartate at position 46, in order to take the inductive effect of the phosphate group into account.

[b] Regular secondary structure elements as observed in PDB #2HPR. Four β-strands are named β-A, β-B, β-C, β-D; three α-helices are named α-A, α-B, α-C.

is detected throughout helix-B. The chemical shift perturbations may be a consequence of a charge–helix macrodipole interaction affecting the electronic environment throughout the helix, or alternatively could be due to a change in the relative populations of helical and nonhelical conformations in this region.

The other NMR parameter that shows significant change in HPr(Ser-P) is the amide exchange rate. The rate at which an amide backbone proton exchanges with solvent depends on its environment: protons that serve as hydrogen bond donors and/or are buried exchange slowly with solvent, whereas protons on the surface of a protein or in regions undergoing dynamical processes such as helix fraying exchange more rapidly. Exchange rates of the amides of residues Leu 44–Leu 53 are all decreased 10–500-fold in HPr(Ser-P), with the largest decreases for the amides of Gly 49 and Val 50. Although the negatively charged phosphate may be expected to cause a decrease in amide exchange rates, this inductive effect should be localized to the amides of residues 46 and 47 (Bai et al., 1993).

Protection factors, which take sequence effects on the intrinsic exchange rates of amides into account ($P = k_{int}/k_{obs}$) provide a means of assessing the effects of structure on amide exchange rates (Bai et al., 1993). As shown in Table 1, the two long α-helices in HPr (helix-A, residues 16–27 and helix-C, residues 70–84) have the highest protection factors in the protein, with log $P \approx 3$ to >4, whereas amide protons in helix-B are only protected in the range of log $P \approx 2$. Because helix-B is barely two turns long, end-fraying effects are likely to dominate its amide exchange rates (Wand et al., 1986). In contrast, the protection factors for helix-B in HPr(Ser-P) are in a range similar to the longer helices, with log $P \geq 3$. Because other NMR parameters indicate that there is no detectable change in the structure of the protein upon phosphorylation, even in the region near Ser 46,

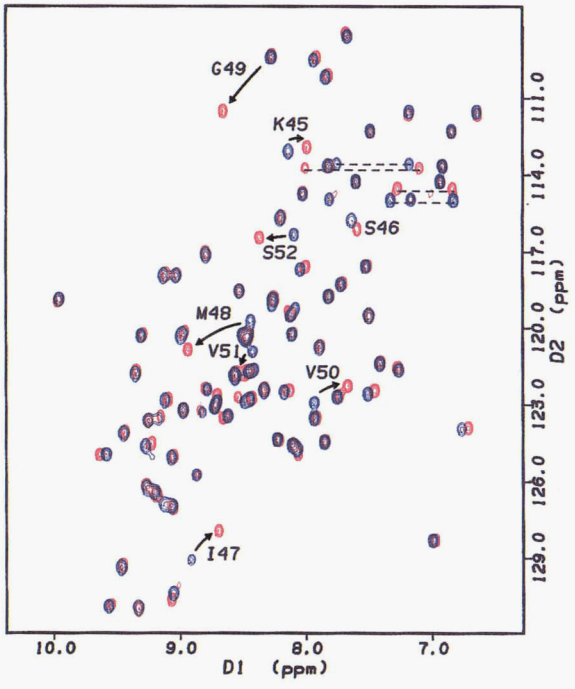

Fig. 2. Overlay of 2D (^{1}H,^{15}N)-HMQC spectra of HPr (blue) and HPr(Ser-P) (red). Amide resonances of residues in the region Leu 44-Ser 52 are indicated; side-chain amide proton resonances (from Asn and Gln residues) are connected by dotted lines.

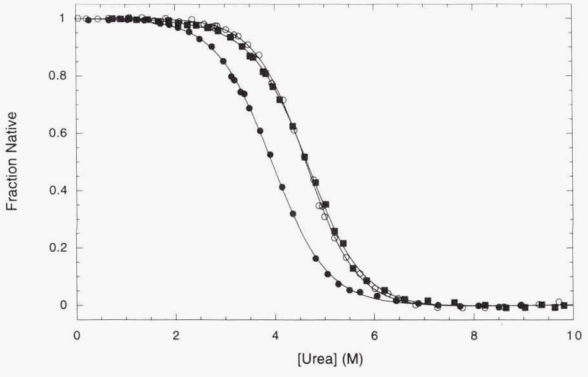

Fig. 3. Comparisons of the unfolding curves for HPr (closed circles), HPr(Ser-P) (open circles), and S46D (closed squares) by urea denaturation. Transitions were monitored by CD spectroscopy and the data normalized as described in the Materials and methods. The best-fit parameters used to construct the curves through the data are shown in Table 2.

the increased protection is likely due to stabilization of the helical structure, whereby the amides spend less time in a state from which exchange with solvent is rapid. Thus, helix-B is stabilized by the phosphate group at its N-terminal end.

NMR spectra of HPr(Ser-P) contain additional evidence of decreased conformational flexibility near Ser 46. Resonances of prochiral methylene protons from three residues that are degenerate in HPr are resolved in HPr(Ser-P): the $C^{\alpha}H$ resonances of Gly 49 and the $C^{\beta}H$ resonances of Asn 43 and Met 48. Chemical shift degeneracy of prochiral protons is often associated with conformational averaging, whereas resolved resonances indicate a more fixed conformation (Wüthrich, 1986). Consistent with this, the ($^3J_{\alpha\beta 2}$, $^3J_{\alpha\beta 3}$) for Asn 43 and Met 48 are (4.6, 10.4 Hz) and (5.6, 9.0 Hz), indicating that these side chains exist within a limited range of conformations in the phosphorylated protein. Also, two NOESY cross peaks have significantly stronger intensity in HPr(Ser-P): Thr 41 $C^{\beta}H$-Lys 42 NH (increased 3.3-fold) and Val 50 $C^{\alpha}H$-Leu 53 NH (increased 5.6-fold).[5] An increase in NOE intensity could be due to a decreased distance between the two protons involved, or to decreased conformational flexibility, causing the protons to spend less time in conformations that do not allow the NOE to occur. Because the NOE involving Val 50 and Leu 53 is consistent with a helical conformation in both HPr and HPr(Ser-P), we favor the second explanation for its increased intensity. Altogether, these observations indicate that the region near Ser 46, from Thr 41 through Leu 53, undergoes less frequent conformational fluctuations in HPr(Ser-P) than in HPr.

The change in local conformational free energy associated with the stabilization of helix-B can be estimated from the amide exchange protection factors, according to the relationship $\Delta\Delta G = -RT \ln[P_{HPr}/P_{HPr(Ser\text{-}P)}]$. Exact values cannot be calculated because the three amide protons in helix-B for which exchange rates could be measured in both forms have exchange half-lives in HPr in the range of 1–10 min, yielding only an upper limit for their protection factors (exchange rates in this range cannot be measured accurately by the exchange measurements performed). Nevertheless, the factors measured for the amides of residues 50, 51, and 53 provide a lower limit estimate of 0.9–1.3 kcal mol^{-1} for the change in conformational free energy for helix-B.

Protein stability studies

The NMR results suggest that phosphorylation of Ser 46 stabilizes helix-B. This conclusion was tested by measuring the conformational stability of HPr and HPr(Ser-P) by analysis of urea denaturation curves and thermal unfolding curves. As a control to establish the electrostatic effect of a negative charge approximately at the position of the phosphate group, a mutant in which aspartic acid replaces Ser 46 (S46D) was also analyzed. The transition, monitored spectroscopically by CD at 222 nm, was fully reversible for all three forms of HPr and can be represented by a simple two-state folding reaction. Figure 3 shows the urea denaturation curves, and Table 2 shows results of the thermodynamic analysis of these data and the thermal unfolding data. Both HPr(Ser-P) and S46D are 0.7–0.8 kcal mol^{-1} more stable than the native form of the protein.[6] Although this $\Delta\Delta G$ is a global value, whereas the estimate based on helix-B

[5] Due to the difficulty in measuring NOESY cross peak intensity accurately, only completely resolved cross peaks were quantified (see the Materials and methods). However, at least one such peak was measured for every residue in the protein and only the two named above, both of which are near the site of phosphorylation, showed a significant difference.

[6] Because the NMR line widths of native HPr and HPr(Ser-P) are indistinguishable, the observed stabilization is not due to a phosphorylation-induced oligomerization.

Table 2. *Analysis of thermodynamic protein stability measurements*[a]

Protein	Urea denaturation		Thermal denaturation		
	C_m (M urea)	$\Delta\Delta G$ (kcal mol^{-1})	T_m (°C)	ΔH_m (kcal mol^{-1})	$\Delta\Delta G$ (kcal mol^{-1})
HPr	3.93 ± 0.05	–	73.6 ± 0.2	59 ± 4	–
HPr(Ser-P)	4.68 ± 0.05	0.79 ± 0.15	77.7 ± 0.3	64 ± 7	0.7 ± 0.2
S46D	4.63 ± 0.05	0.74 ± 0.15	77.5 ± 0.3	63 ± 6	0.7 ± 0.2

[a] Changes in ΔG for each variant, compared to the wild-type protein ($\Delta\Delta G$) for the urea denaturation curves were calculated by: $\Delta\Delta G = \langle m \rangle \cdot \Delta C_m$, where $\langle m \rangle$ = 1,050 ± 50 cal mol^{-1} M^{-1}, the average m-value for *B. subtilis* HPr (Scholtz, 1995) and ΔC_m is the difference in midpoint of the transition relative to wild-type protein. The changes in ΔG from the analysis of the thermal unfolding data were determined by the relationship: $\Delta\Delta G = \Delta T_m \cdot \Delta H_m(\text{wt})/T_m(\text{wt})$, with T expressed in Kelvin (Becktel & Schellman, 1987).

protection factors of ~1 kcal mol^{-1} is a local value, the agreement between the two different measurements suggests that each are reporting the same event, namely, stabilization of helical structure by phosphorylation of Ser 46.

Structure of HPr(Ser-P)

Because the NMR results show the structure of HPr(Ser-P) to be virtually identical to HPr, the structure of HPr(Ser-P) was modeled from the crystal structure of HPr, which is a good model for the B-helix-containing conformation. Helix-B in HPr, HPr(Ser-P), and S46D (Liao & Herzberg, 1994) is shown in Figure 4. An earlier modeling study based on the crystal structure of HPr revealed that addition of a phosphate to Ser 46 could be accomplished without major structural perturbations, although it was suggested that a 60° rotation in χ_1 would be required to avoid steric clashes (Herzberg et al., 1992). The NMR results indicate that the χ_1 of Ser 46 remains in the *trans* conformation and therefore clashes must be avoided through adjustments to χ_2. As shown in Figure 4, the negatively charged phosphate group sits near the N-terminus of helix-B, in a position to allow for a favorable electrostatic interaction. The *trans* rotamer maintains the uncharged Oγ of the Ser-P in H-bond geometry to the amide of Gly 49, similar to the position of the Oγ in the unphosphorylated form and to one of the aspartate carboxylate oxygens in S46D. Within the constraints of a *trans* χ_1 rotamer, the only potential H-bond involving a phosphate oxygen and a main-chain amide identified through modeling is to the amide of Ile 47. However, given the upfield shift of the Ile 47 NH resonance and the minimal increase in protection factor observed for this residue, the NMR data do not support this proposed interaction. Thus, although Ser 46-P is in the N-cap position of helix-B, addition of the phosphoryl group does not result in new H-bonds at the N-terminal end of the helix, but rather its interaction with the helix must be mainly via a charge–helix macrodipole, with a net result that the protein is stabilized by ~0.8 kcal mol^{-1}.

Discussion

Comparison with other phosphorylated proteins

How do the results for HPr compare to the other examples of phosphoserine-containing protein structures? Similar to HPr, IDH and cAPK have Ser-P residues at the −1 position of an α-helix and the Ser-P residue in GP is at the N-terminus of a 3_{10} helix (Fig. 5). Similar to HPr(Ser-P), none of the phosphate groups are directly involved in hydrogen bonds with main-chain atoms in the helices. It appears that the Ser-P side chain may be too bulky to act as an effective N-capping residue and instead exerts its effects through a charge–helix macrodipole interaction.

We have recently reported the effects of phosphorylation of His 15 on structural features of HPr (Rajagopal et al., 1994). His 15 is also at the −1 position of a helix and the phosphohistidine residue serves as an N-cap for helix-A, making hydrogen bonds to main-chain amides of residues 16 and 17. We also noted that the phosphohistidine residue in enzyme IIA^{glc} from *Escherichia coli* appears to interact with the N-terminal end of a short helix, although in this case the phosphorylated residue

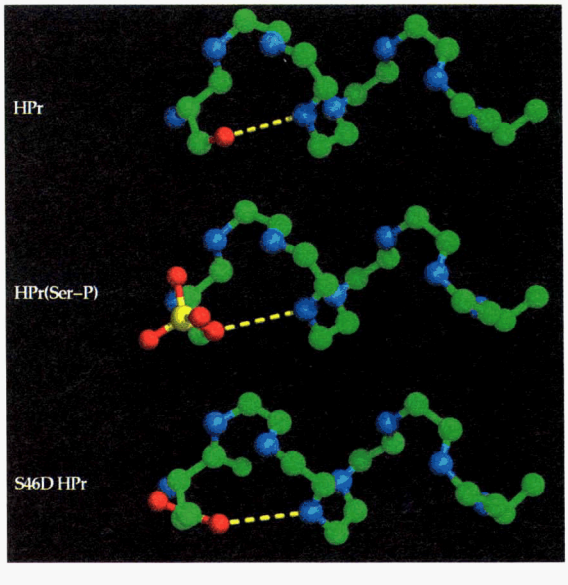

Fig. 4. Position of the side chain of residue 46, relative to helix-B in HPr (Herzberg et al., 1992; PDB 2HPR), HPr(Ser-P) (see the Materials and methods), and the mutant S46D (Liao & Herzberg, 1994; PDB 1SPH). Nitrogens are blue, carbons are green, oxygens are red, and phosphorus is yellow. Each structure predicts a hydrogen bond involving the backbone amide group of Gly 49 and an oxygen from residue 46 (see text).

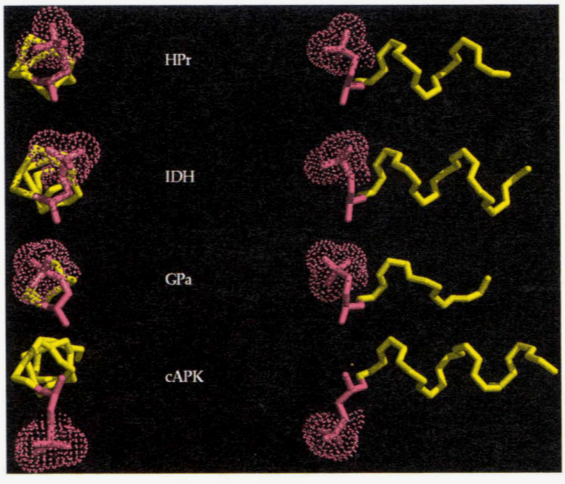

Fig. 5. Examples of serine-phosphate residues at the N-termini of helices. Dotted spheres represent the van der Waals surface of the phosphate group. The four structures were superimposed using backbone atoms only for the Ser-P residue plus the next three residues in the structure. Two views are shown. On the left is a view down the helical axis and on the right, the previous view has been rotated 90°. HPr(Ser-P), residues 46–53, as modeled in this study. IDH(Ser-P), residues 113–123 (PDB 4ICD). The phosphate group is situated in a similar conformation relative to the helix as in the HPr(Ser-P) model. There are no hydrogen bond contacts between the phosphoryl oxygens and main-chain atoms. GPa(Ser-P), residues 14–19 (PDB 1GPA). cAPK(Ser-P), residues 10–20 (PDB 1APM). The phosphate group points away from the helix axis, making no hydrogen bond contacts with main-chain atoms. The extended conformation of this Ser-P residue is likely due to the proximity of two other negatively charged side chains in the first turn of the helix, Glu 11 and Glu 13.

is not in a canonical N-cap position. The phosphohistidine residue in succinyl-CoA synthetase from *E. coli* interacts with the N-termini of two α-helices in the crystal structure (Wolodko et al., 1994). Taken together, these observations strongly suggest that a major motif for phosphorylated proteins is one in which the phosphate group sits at the N-terminal end of a helix. A similar motif is observed in many noncovalent protein–phosphate interactions (Hol et al., 1978; Hol, 1985).

Implications for HPr function

Our goal is to understand how the physical effects of phosphorylation lead to unique functional consequences. Phosphorylation of Ser 46 prevents the interaction of HPr with enzyme I, sugar-specific IIA proteins, and possibly with other protein domains (Reizer et al., 1984, 1992; Deutscher et al., 1995; Ye & Saier, 1995). Although the enzyme I-binding site on *B. subtilis* HPr has not yet been determined, it has recently been shown to be indistinguishable from the enzyme IIA^{glc}-binding site on HPr in the analogous *E. coli* proteins (van Nuland et al., 1995). The enzyme IIA^{glc} recognition site on HPr has been mapped by chemical shift perturbations (Chen et al., 1993) and amide exchange rate perturbations (P. Rajagopal & R.E. Klevit, unpubl. results) to a region that includes helix-B. These studies place Ser 46 at the edge of the protein–protein interaction surface, which consists mainly of hydrophobic and positively charged residues. Given the results reported here that phosphorylation of Ser 46 is not accompanied by a global conformational change, the phosphate group must exert its effect through a change in surface electrostatics at the site of target protein binding, or a direct steric hindrance, or a combination of both effects.

Implications for mechanism of action of protein phosphorylation

In summary, proteins that undergo regulatory serine phosphorylation may be classified into two types: those that undergo a global conformational change upon phosphorylation and those that do not. Like IDH, HPr is the second example of a protein in which a regulatory serine phosphorylation is *not* accompanied by a change in conformation. Our solution measurements detect a stabilizing effect of phosphorylation in the absence of conformational change. An emerging picture is one in which covalent phosphate groups in proteins interact with the N-terminal ends of α-helices. We hypothesize that, if a serine is near the N-terminal end of a helix, its phosphorylation will likely not be accompanied by a conformational change, but may instead result in a modest stabilization of the protein that may be reflected as a change in dynamical properties near the end of the helix. Dynamical fluctuations of the polypeptide may be critical for binding in the active site of a kinase, especially in cases where the phosphorylation site is helical. The structure of an inhibitory peptide bound to the active site of cAPK is that of an extended chain (Zheng et al., 1993), implying that a helical site must undergo a conformational change in the active site, even though the starting and ending structures are similar. Intriguingly, disorder or flexibility is a property of nonhelical phosphorylation sites as well: phosphorylation of GP is accompanied by a disorder-to-order transition of the polypeptide near Ser 14; the region N-terminal to and including Ser 10 in cAPK is disordered in several crystal structures; and the nonregulatory phosphorylation site (Ser 80) in cystatin has high flexibility (Dieckmann et al., 1993). In conclusion, we have characterized the effects of phosphorylation on protein structure and stability in solution, adding important new insight to the structural database of proteins containing regulatory Ser-P residues and showing that properties other than conformational rearrangements can be affected by this ubiquitous regulatory mechanism.

Materials and methods

Protein preparation

B. subtilis HPr and HPr(Ser-P) were prepared as previously described (Wittekind et al., 1989, 1992; Reizer et al., 1992) and complete phosphorylation was confirmed by electrospray mass spectrometry. NMR samples were prepared as described (Wittekind et al., 1992). Final concentrations were 1.5–2.0 mM protein, 50 mM potassium phosphate, 0.2 mM EDTA, and 2 mM sodium azide.

NMR spectroscopy

NMR experiments were performed on a Bruker AM500 or DMX500 spectrometer using standard pulse sequences, at 30 °C unless otherwise noted. Resonances of HPr(Ser-P) were assigned by comparison to analogous spectra of HPr and confirmed by TOCSY (75 ms mixing time) and sequential NOESY (75 ms and 100 ms mixing times) connectivities.

NOESY volumes were measured in spectra corrected for the shape of the excitation profile of the spin-echo pulse sequence used for water suppression. Volume ratios for 108 well-resolved cross peaks involving amide protons were measured and corrected for differences in protein concentration, yielding an average ratio for HPr(Ser-P)/HPr of 1.0 (SD = 0.6). A cross peak was deemed to be significantly different in the two forms if the ratio was more than 2 SD from 1.0.

Exchange rates of slowly exchanging amide protons were determined from a series of six magnitude ^{1}H COSY spectra collected at 15 °C, pH* 6.9 (uncorrected meter reading) on samples that had been dissolved in D_2O immediately before data collection. The first spectrum was collected at 24.5 min and the last spectrum at 208.5 min following dissolution. NH-C$^\alpha$H cross peak volumes were measured and plots of volumes as a function of time were fit to single exponentials to determine exchange half-lives.

Exchange rates of fast-exchanging amides were determined using volumes from magnitude COSY spectra collected with and without solvent presaturation at 3 pH values (pH 6.5, 6.9, and 7.3). A 1-1 spin-echo pulse sequence was used to suppress H_2O in spectra collected without presaturation (Spera et al., 1991).

Protein denaturation studies

Urea denaturation experiments on HPr were performed as described (Scholtz, 1995). CD at 222 nm was used to monitor the equilibrium unfolding data using an Aviv 62DS spectropolarimeter equipped with a temperature control and stirring unit. The urea denaturation curves at 30 °C were obtained with urea solutions prepared fresh daily in buffered solutions containing 50 mM potassium phosphate at pH 7.0. The concentration of the urea stock solution was determined by refractive index measurements (Pace, 1986). In order to compare directly the results for the different proteins, urea denaturation curves were performed for all proteins using the same urea solutions on the same day. These were repeated on four separate days to afford a measure of the uncertainty in each calculated parameter.

A complete description of the data analysis performed on the urea and thermal denaturation experiments has been described (Scholtz, 1995). The changes in ΔG for each variant, compared to the wild-type protein ($\Delta\Delta G$) for the urea denaturation curves were calculated by: $\Delta\Delta G = \langle m \rangle \cdot \Delta C_m$, where $\langle m \rangle = 1{,}050 \pm 50$ cal mol^{-1} M^{-1}, the average m-value for *B. subtilis* HPr (Scholtz, 1995) and ΔC_m is the difference in midpoint of the transition relative to wild-type protein. The changes in ΔG from the analysis of the thermal unfolding data were determined by the relationship described by Becktel and Schellman (1987): $\Delta\Delta G = \Delta T_m \cdot \Delta H_m(\text{wt})/T_m(\text{wt})$, with T expressed in Kelvin. Each of these methods assumes a two-state unfolding reaction. The analysis of the urea denaturation curves also assumes a linear relationship between the free energy of folding and the molar urea concentration (linear extrapolation method), whereas the analysis of the thermal unfolding curves assumes a constant ΔC_p for the proteins.

Structural modeling

HPr(Ser-P) was modeled using INSIGHT (Biosym, Inc.) from the crystal coordinates (PDB 2HPR) by substituting phosphoserine at position 46 and adjusting the side chain to alleviate steric clashes. Molecular graphics images in Figures 1, 4, and 5 were produced using the MidasPlus program (Bash et al., 1983; Ferrin et al. 1988; Huang et al., 1991) from the Computer Graphics Laboratory, University of California, San Francisco (supported by NIH RR-01081)

Acknowledgments

This work was supported by NIH RO1 DK35187 (R.E.K.), NIH R29 GM52483 (J.M.S.), and NIH 5RO1 AI21702 and NIH 2RO1 AI14176 (M.H.S.). We thank Walt Massefski (Pfizer Center Research, Groton, Connecticut) for collecting natural abundance ^{13}C NMR spectra, Wim Hol and Mia Schmiedeskamp for critical reading of the manuscript, and Bryan Jones for preparation of Figures 1, 4, and 5.

References

Bai Y, Milne JS, Mayne L, Englander SW. 1993. Primary structure effects on peptide group hydrogen exchange. *Proteins Struct Funct Genet 17*: 75-86.

Barford D, Johnson LN. 1989. The allosteric transition of glycogen phosphorylase. *Nature 340*:609-616.

Bash PA, Pattabiraman N, Hunag CC, Ferrin TE, Langridge R. 1983. Van der Waals surfaces in molecular modeling: Implementation with real-time computer graphics. *Science 222*:1325-1327.

Becktel WJ, Schellman JA. 1987. Protein stability curves. *Biopolymers 26*: 1859-1877.

Chen Y, Reizer J, Saier MH Jr, Fairbrother WJ, Wright PE. 1993. Mapping of the binding interfaces of the proteins of the bacterial phosphotransferase system, HPr and IIAglc. *Biochemistry 32*:32-37.

Cox S, Radzio-Andzelm E, Taylor SS. 1994. Domain movements in protein kinases. *Curr Opin Struct Biol 4*:893-901.

Deutscher J, Kuster E, Bergstedt U, Charrier V, Hillen W. 1995. Protein kinase-dependent HPr/CcpA interaction links glycolytic activity to carbon catabolite repression in gram-positive bacteria. *Mol Microbiol 15*: 1049-1053.

Deutscher J, Reizer J, Fischer C, Galinier A, Saier MH Jr, Steinmetz M. 1994. Loss of protein kinase-catalyzed phosphorylation of HPr, a phosphocarrier protein of the phosphotransferase system, by mutation of the ptsH gene confers catabolite repression resistance to several catabolic genes of *Bacillus subtilis*. *J Bacteriol 176*:3336-3344.

Dieckmann T, Mitschang L, Hofmann M, Kos J, Turk V, Auerswald EA, Jaenicke R, Oschkinat H. 1993. The structures of native phosphorylated chicken cystatin and of a recombinant unphosphorylated variant in solution. *J Mol Biol 234*:1048-1059.

Ferrin TE, Huang CC, Jarvis LE, Langridge R. 1988. The MIDAS display system. *J Mol Graphics 6*:13-27.

Herzberg O, Reddy P, Sutrina S, Saier MH Jr, Reizer J, Kapadia G. 1992. Structure of the histidine-containing phosphocarrier protein HPr from *Bacillus subtilis* at 2.0-Å resolution. *Proc Natl Acad Sci USA 89*:2499-2503.

Hol WG, Van Duijnen PT, Berendsen HJ. 1978. The alpha-helix dipole and the properties of proteins. *Nature 273*:443-446.

Hol WG. 1985. The role of the alpha-helix dipole in protein function and structure. *Prog Biophys Mol Biol 45*:149-195.

Huang CC, Petterson EF, Klein TE, Ferrin TE, Langride R. 1991. Conic: A fast renderer for space-filling molecules with shadows. *J Mol Graphics 9*:230-236.

Hurley JH, Dean AM, Thorsness PE, Koshland DE Jr, Stroud RM. 1990. Regulation of isocitrate dehydrogenase by phosphorylation involves no long-range conformational change in the free enzyme. *J Biol Chem 265*: 3599-3602.

Krebs EG, Fischer EH. 1956. The phosphorylase *b* to *a* converting enzyme of rabbit skeletal muscle. *Biochim Biophys Acta 20*:150-157.

Liao DI, Herzberg O. 1994. Refined structures of the active Ser 83 → Cys and impaired Ser 46 → Asp histidine-containing phosphocarrier proteins. *Structure 2*:1203-1216.

Pace CN. 1986. Determination and analysis of urea and guanidine hydrochloride denaturation curves. *Methods Enzymol 131*:266-280.

Postma PW, Lengeler JW, Jacobson GR. 1993. Phosphoenolpyruvate:carbohydrate phosphotransferase systems of bacteria. *Microbiol Rev 57*: 543-594.

Rajagopal P, Waygood EB, Klevit RE. 1994. Structural consequences of histidine phosphorylation: NMR characterization of the phosphohistidine

form of histidine-containing protein from *Bacillus subtilis* and *Escherichia coli*. *Biochemistry 33*:15271–15282.

Reizer J, Novotny MJ, Hengstenberg W, Saier MH Jr. 1984. Properties of ATP-dependent protein kinase from *Streptococcus pyogenes* that phosphorylates a seryl residue in HPr, a phosphocarrier protein of the phosphotransferase system. *J Bacteriol 160*:333–340.

Reizer J, Sutrina SL, Wu LF, Deutscher J, Reddy P, Saier MH Jr. 1992. Functional interactions between proteins of the phosphoenolpyruvate:sugar phosphotransferase systems of *Bacillus subtilis* and *Escherichia coli*. *J Biol Chem 267*:9158–9169.

Scholtz JM. 1995. Conformational stability of HPr: The histidine-containing phosphocarrier protein from *Bacillus subtilis*. *Protein Sci 4*:35–43.

Spera S, Ikura M, Bax A. 1991. Measurement of the exchange rates of rapidly exchanging amide protons: Application to the study of calmodulin and its complex with a myosin light chain fragment. *J Biomol NMR 1*: 155–165.

van Nuland NA, Boelens R, Scheek RM, Robillard GT. 1995. High-resolution structure of the phosphorylated form of the histidine-containing phosphocarrier protein HPr from *Escherichia coli* determined by restrained molecular dynamics from NMR-NOE data. *J Mol Biol 246*:180–193.

Wand AJ, Roder H, Englander SW. 1986. Two-dimensional ^{1}H NMR studies of cytochrome *c*: Hydrogen exchange in the N-terminal helix. *Biochemistry 25*:1107–1114.

Wittekind M, Rajagopal P, Branchini BR, Reizer J, Saier MH Jr, Klevit RE. 1992. Solution structure of the phosphocarrier protein HPr from *Bacillus subtilis* by two-dimensional NMR spectroscopy. *Protein Sci 1*:1363–1376.

Wittekind M, Reizer J, Deutscher J, Saier MH, Klevit RE. 1989. Common structural changes accompany the functional inactivation of HPr by seryl phosphorylation or by serine to aspartate substitution. *Biochemistry 28*: 9908–9912.

Wolodko WT, Fraser ME, James MN, Bridger WA. 1994. The crystal structure of succinyl-CoA synthetase from *Escherichia coli* at 2.5 Å resolution. *J Biol Chem 269*:10883–10890.

Wüthrich K. 1986. *NMR of proteins and nucleic acids*. New York: John Wiley & Sons, Inc.

Ye JJ, Reizer J, Cui X, Saier MH Jr. 1994. Inhibition of the phosphoenolpyruvate:lactose phosphotransferase system and activation of a cytoplasmic sugar-phosphate phosphatase in *Lactococcus lactis* by ATP-dependent metabolite-activated phosphorylation of serine 46 in the phosphocarrier protein HPr. *J Biol Chem 269*:11837–11844.

Ye JJ, Saier MH Jr. 1995. Purification and characterization of a small membrane-associated sugar phosphate phosphatase that is allosterically activated by HPr(Ser-P) of the phosphotransferase system in *Lactococcus lactis*. *J Biol Chem 270*:16740–16744.

Zheng J, Knighton DR, Ten Eyck LF, Karlsson R, Xuong N, Taylor SS, Sowadski JM. 1993. Crystal structure of the catalytic subunit of cAMP-dependent protein kinase complexed with MgATP and peptide inhibitor. *Biochemistry 32*:2154–2161.